Reconnectable Sub-5 nm Nanogaps in Ultralong Gold Nanowires

3 AUTHORS, INCLUDING:

Chengxiang Xiang
California Institute of Technology

38 PUBLICATIONS   **835** CITATIONS

SEE PROFILE

Reginald M Penner
University of California, Irvine
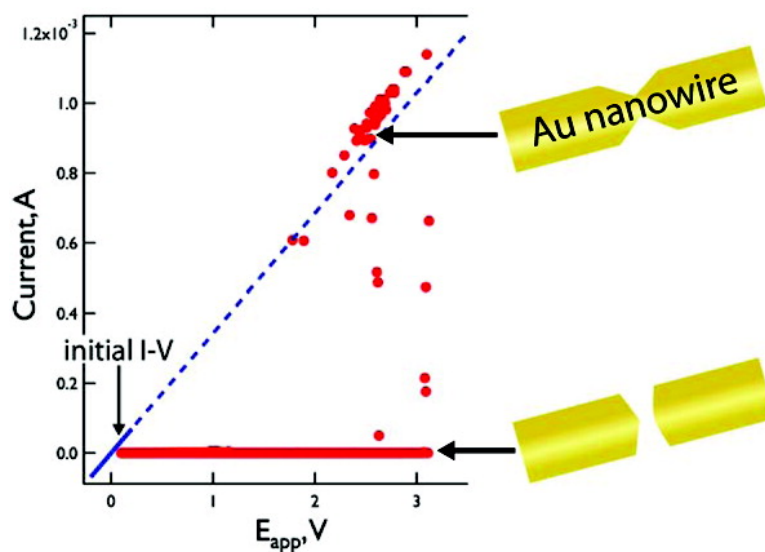
63 PUBLICATIONS   **2,370** CITATIONS

SEE PROFILE

Letter

Reconnectable Sub-5 nm Nanogaps in Ultralong Gold Nanowires

Chengxiang Xiang, Jung Yun Kim, and Reginald M. Penner

More About This Article

Additional resources and features associated with this article are available within the HTML version:

- Supporting Information
- Access to high resolution figures
- Links to articles and content related to this article
- Copyright permission to reproduce figures and/or text from this article

View the Full Text HTML

Reconnectable Sub-5 nm Nanogaps in Ultralong Gold Nanowires

Chengxiang Xiang, Jung Yun Kim, and Reginald M. Penner*

Department of Chemistry, University of California, Irvine, California 92697-2025

ABSTRACT

A protocol is described for forming reconnectable sub-5 nm nanogaps in single ultralong (>100 μm) gold nanowires fabricated by lithographically patterned nanowire electrodeposition (LPNE). During an initial computer-controlled electromigration process, gold nanowires with a rectangular cross-section were transformed by the formation of a constriction at a single point along the 250 μm length of the nanowire, and within this constriction a nanogap of width <5 nm. After this initial nanogap formation, 42% (19 of 45) of the gaps could be reconnected by applying a voltage ramp, restoring the electrical resistance of the original nanowire to within 10%. The voltage threshold for nanogap reconnection was narrowly distributed across multiple wires and nanogaps and in the range from 2 to 3 V. Using voltage programming, it was possible to cycle between the open and closed states for some nanogaps more than 100 times. We propose that the mechanism for reconnection involves the field evaporation of gold, qualitatively as observed previously for metal transfer from the tip of a scanning tunneling microscope.

Nanometer scale gaps in metal nanowires and in microfabricated "bowtie" structures can be formed by electromigration for applications in molecular electronics[1–4] and plasmonics.[5,6] Sub-5 nm nanogaps have been produced by direct voltage ramp up,[7–9] feed-back controlled voltage ramp up[10–12] and current-controlled electromigration.[2] Nanowire structures and bow-tie structures have both been used to study the electromigration process by real time scanning electron microscopy (SEM)[13] and transmission electron microscopy (TEM).[14–16] In this letter, we report the fabrication of a sub-5 nm nanogap within an ultralong (≈250 μm) gold nanowire by a feed-back controlled electromigration process. This feedback algorithm permitted quasi-symmetrical nanogap structures to be formed. A surprising attribute of these nanogaps is that with a success rate of 42% they can be reconnected by ramping the voltage across the gap to ≈3 V, and for some nanogaps it was possible to cycle between the open and closed states by voltage programming more than 100 times. In this letter, we describe the algorithm used to produce these these nanogaps, we report the electrical properties of representative nanogaps and we characterize the reconnection process.

For the investigations reported here, a 250 μm length of a single gold nanowire was electrically isolated between two nickel contacts (Figure 1a,b) and supported on a glass substrate. These gold nanowires, fabricated using the lithographically patterned nanowire electrodeposition (LPNE) method,[17–20] had total lengths of up to 1 cm and a rectangular cross-section with typical widths of 110–500 nm and heights of 40 nm (Figure 1c). The electrical contact seen in Figure
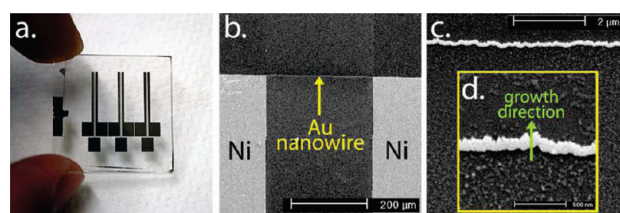

Figure 1. (a) Optical micrograph of the device used to study the electromigration of long gold nanowires. (b) SEM image of a single gold nanowire that was electrically contacted by two nickel pads. (c,d) Low and higher magnification SEM images of a typical gold nanowire used for these investigations.

1b was obtained by lithographically patterning the same evaporated nickel layer used to direct nanowire growth in the LPNE process, thereby ensuring the electrical integrity of the nickel−gold contact.[21] PELCO colloidal silver paste was applied onto the nickel pad and air-dried overnight before any electrical measurement. The potentials of the nickel contacts were controlled by a computer-controlled SourceMeter (Keithley 2400) during the electromigration, electrical characterization, and reconnection processes.

Nanogaps were produced using a programmed voltage algorithm that was controlled by a Labview program. The process flow for this program (Figure 2a) involved (1) the application of an initial voltage bias ($E_{app,i}$ = 10−100 mV) and the measurement of an initial wire resistance, R_0, (2) E_{app} was then increased in a ramp at a rate of 5 mV/s, and the wire resistance was simultaneously measured, (3) when the resistance change ratio ($R - R_0)/R_0$ exceeded a predefined threshold (typically 1.5%), a new reference resistance value was measured at $E_{app} = 0.95E_{app,i}$ and the cycle was repeated.
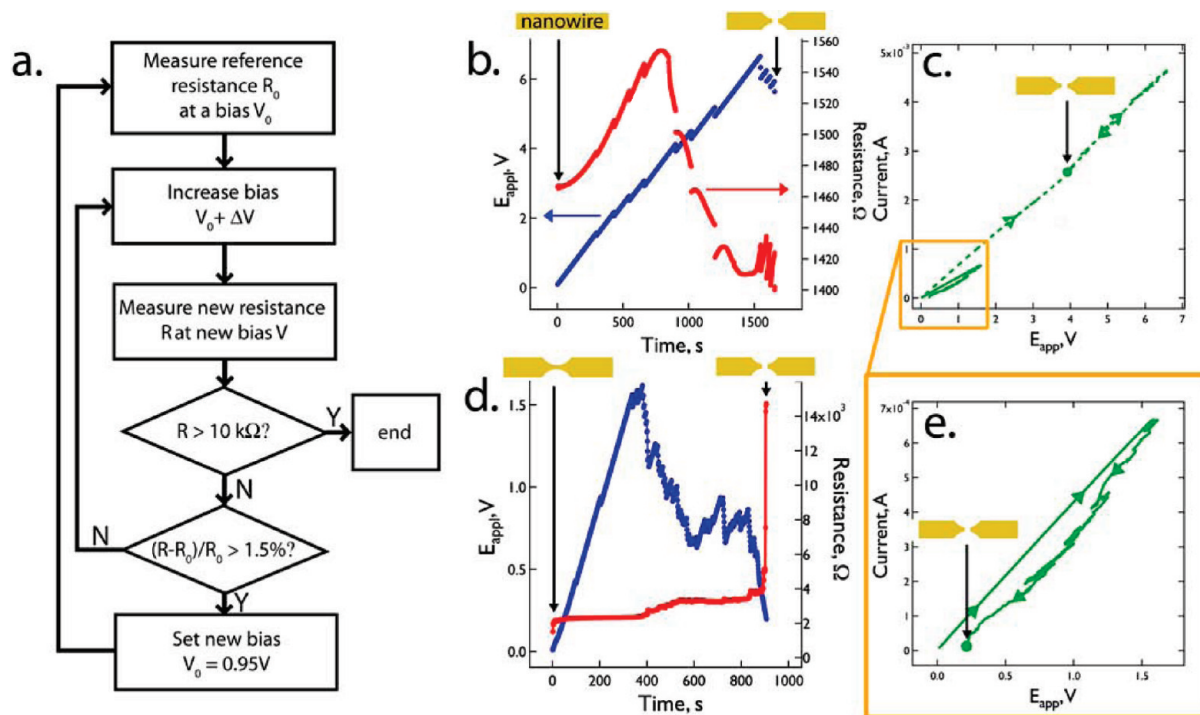
Figure 2. (a) Flowchart for the Labview algorithm governing the feedback-controlled electromigration process. (b) The applied potential (E_{app}) and the nanowire resistance (R) as a function of time for the initial formation of a nanogap in a fresh nanowire. (c) The current−voltage trace for the electromigration process for the fresh nanowire (dotted green line) and reconnected nanowire (solid green line). The arrow indicates the nanowire failure point. (d) The applied potential (E_{app}) and the nanowire resistance (R) as a function of time for the reconnected nanowire. (e) The current−voltage trace for the electromigration process for the reconnected nanowire. The arrow indicates the failure point.

This program terminated when the formation of a nanogap was signaled by the measurement of $R > 10$ kΩ.

A distinctive time-dependence of E_{app} and R are seen during this initial formation of a nanogap in a fresh nanowire. These data are shown for a typical 450×40 nm wire in Figure 2b,c. E_{app} increases approximately linearly during the entire $1000-2000$ s required for nanogap formation, until within 200 s of nanogap formation E_{app} decreases suddenly by $10-20\%$ (Figure 2b). For much of this period, E_{app} is less than 1.5 V and little hysteresis in E_{app} or R (Figure 2b) is observed. If the electromigration process is stopped while $E_{app} < 1.5$ V and the voltage is reduced to its initial value ($E_{app,i} = 10-100$ mV), the initial resistance of the nanowire is recovered. We conclude that no morphological change in the wire has occurred at $E_{app} < 1.5$ V, and this conclusion is supported by SEM images of the nanowire acquired at this juncture (data not shown).

R, in contrast, increases initially but peaks at $500-1000$s and then decreases smoothly by $10-20\%$ prior to nanogap formation (Figure 2b). The resulting trajectory in current versus E_{app} (Figure 2c) is ohmic, but the role-over of the current seen at the midpoint of the electromigration means that the system retraces the ohmic $I-V$ back down to ≈ 5 V (for the experiment of Figure 2b,c) before breaking. This resistance decrease is likely the result of grain growth accelerated by Joule heating of the nanowire. Above 1.5 V, the resistance change is no longer reversible and thermally activated electromigration competes with wire annealing and grain growth with both processes altering the wire morphol-

ogy up to the failure point. We demonstrate below that this morphological change involves the formation of a constriction in the nanowire where the nanogap forms, and this constriction concentrates the ohmic drop along the wire, having implications for its behavior in subsequent reconnection and reopening operations. Our success rate for producing nanogaps using the algorithm of Figure 2a was 68% (45 for 66 attempts) but all "failed" attempts represented nanowires that were completely destroyed by static electrical discharges.

After the formation and electrical characterization of the nanogap, its morphology was investigated using scanning electron microscopy (SEM). It is worth noting here that while gold nanowires after electromigration retain mechanical integrity, electromigrated wires showed an increased vulnerability to destruction by static electrical discharges leading to loss of long, $\approx 1-20$ μm, segments of nanowire from the surface. A compliment of antistatic measures must be employed to guard against this. SEM images of nanogaps (Figure 3) show that the nanowire in the vicinity of the nanogap has lost its characteristic flat profile produced by the LPNE fabrication. This morphological change is consistent with the wire heating that must accompany the electromigration process in these ultralong nanowires. To a first approximation, the nanogaps formed during this study were uniformly distributed along the 250 μm electrically isolated length of the nanowire (Figure 4). The gap size cannot be accurately measured from SEM images like those shown in Figure 2, but for many nanogaps a tunneling current
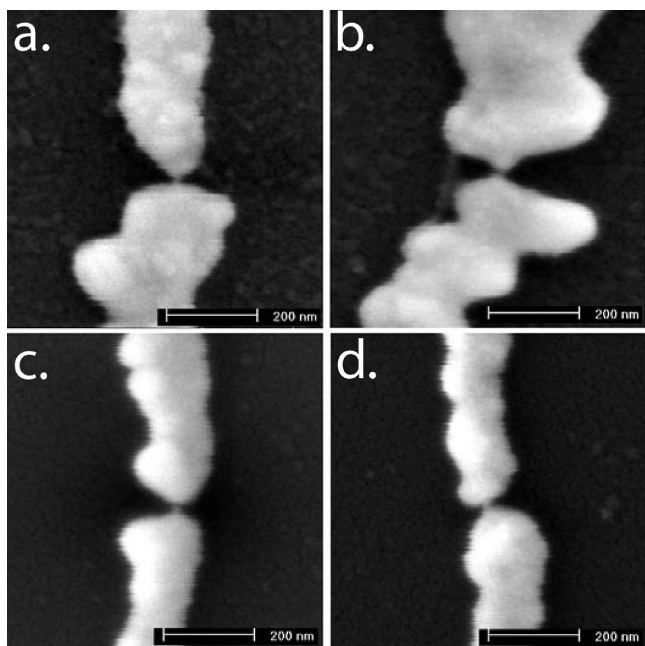
Figure 3. (a−d) High magnification SEM images of nanogaps formed using the algorithm of Figure 1a.
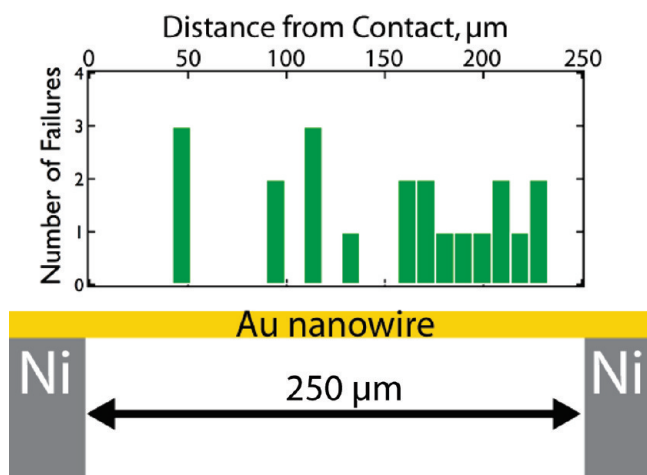
Figure 4. Nanogap location distribution along the 250 μm length of the nanowire, relative to one nickel contact.

can be measured and its voltage dependence affords an estimate of the gap width. For example, the characteristic tunneling $I-V$ curve of a typical nanogap (Figure 6b, broken line) was obtained by scanning the applied voltage from −0.2 to 0.2 V at room temperature in air. The solid line is a least-squares fit to this $I-V$ trace using the Simmons tunneling model[22]

$$I = \frac{k_1 A}{s^2}[x^2 e^{-k_2 s x} - y^2 e^{-k_2 s y}] \quad (1)$$

where $x = [\varphi - (V/2)]^{1/2}$, $y = [\varphi + (V/2)]^{1/2}$, $k_1 = 6.32 \times 10^{10}$ V s^{-1}, $k_2 = 1.025$ $J^{-1/2}$. The variables s, A, and φ are the gap size, the emission area, and the barrier height, respectively. This model is valid for the bias voltage range: $0 < V < \varphi$. From the fitting curve, we obtained the nanogap size for this particular device as $s = 1.6$ nm. Other parameters are $A = 1.4 \times 10^{-15}$ cm^2 and $\varphi = 0.196$ eV, which are similar to the values obtained previously for gold nan-

ogaps.[23,24] Twenty-one percent of the nanogaps we created showed tunneling behavior with a mean gap width of 2.0 (±1.4) nm. A second, indirect indicator of the gap width supporting a value in the 5 nm range is the low voltage threshold for reconnection (<3 V) since the reported threshold field for reconnection in related STM experiments (see discussion below) has been on the order of 1 V/Å.[26,27]

Nanogaps prepared by the feedback-controlled electromigration program can be reconnected by application of a voltage ramp to the broken nanowire and we return to the details of the reconnection process in the next paragraph. Once this nanogap is reconnected, it may be opened a second time by subjecting it to the same algorithm used in its initial preparation (Figure 2a). But dramatically different electrical metrics of E_{app}, I, and R versus times are seen during this process (Figure 2d,e) compared with the first gap formation process (Figure 2b,c). Two major differences are the following: (1) The reconnected nanowire fails at a lower voltage bias. Specifically, wire failure finally occurs at E_{app} of just 200−300 mV after peaking at 1.5 V (Figure 2d). (2) No regime of decreasing resistance attributed to thermal annealing and grain growth is observed. Instead, the resistance increases monotonically (Figure 2d), just as usually seen in prior nanogap formation experiments involving bow-tie structures.[10,12] The I versus E_{app} trajectory for this nanogap reformation (Figure 2e) also closely resembles that reported previously by others for bow-tie systems.[10,12] Thus, the disparate behavior seen for the first nanogap formation compared to the reconnection process (Figure 2a−d) is the logical consequence of a different initial state of the nanowire; the fresh LPNE nanowire lacks the bow-tie-like constriction formed during the first electromigration.

Nanogap reconnection was achieved by ramping the voltage from 0 V at 100 mV/s while monitoring the wire resistance. This applied bias was removed when a threshold resistance of 20 KΩ or less was observed, signaling that reconnection was complete. Of the 45 nanogaps that were not destroyed by static electrical discharge, 19 (42%) were reconnected using this procedure. After each reconnection, the nanowire was subjected to the feedback-controlled electromigration algorithm (Figure 2a) and the pre-existing "healed" nanogap was reopened. Shown in Figure 5a is the current versus voltage response for a nanogap as it was reconnected 52 consecutive times. At the beginning of each reconnection attempt, the nanogap is initially at open circuit and a bias of 10 mV to 100 mV is applied to it. Then the voltage was increased (horizontal red trace) until a current was observed, indicated by the red data points distributed at currents ranging from 0.05 to 1.1 mA. Other nanogaps were successfully reconnected more than 100 times. The red data points arrayed at nonzero currents in Figure 5a map out a voltage threshold for reconnection that is narrowly distributed and centered at 2.5 V. A histogram of this reconnection voltage threshold for 10 different nanogaps in 10 different gold nanowires (Figure 5b) shows a mean reconnecting voltage threshold of 2.6 ± 0.6 V. It is unclear why a nanogap that is initially reconnectable fails to reconnect after some number of trials. To first order, we can assume that the reconnection voltage is positively correlated with the gap
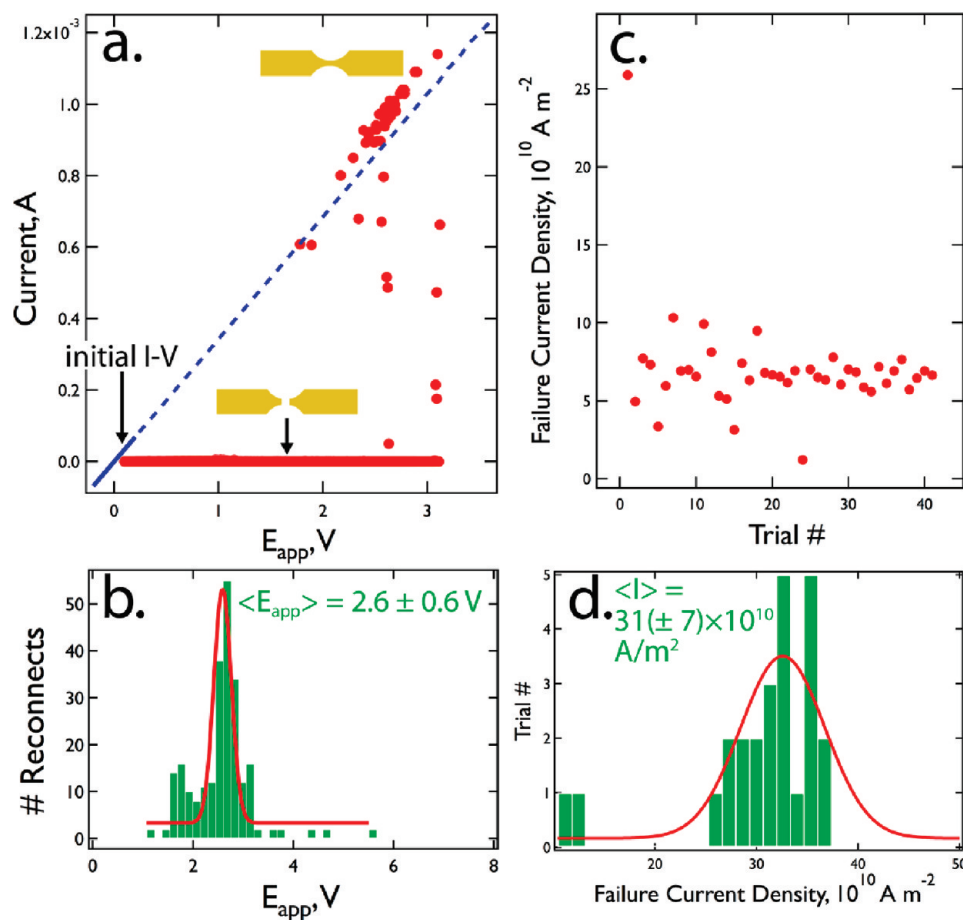
Figure 5. (a) I as a function of E_{app} plotted during the reconnection process. The dashed blue line is an linear extrapolation of the initial $I-V$ curve measured for the initial fresh nanowire. (b) Histogram of the reconnection threshold voltage for 10 different nanowires. (c) Failure current density as a function of sequential breaks for a particular gold nanowire. (d) Histogram of the failure current density for fresh gold nanowires.

**Table 1.** Observed Failure Current Density For Gold Nanowires

author	dimensions	crystallinity	failure current density
Durkan et al.[a]	W: 25−850 nm H: 20 nm L: 1 um	polycrystalline	1.8×10^{12} A m^{-2}
Aherne et al.[b]	Dia: 66−117 nm L: 353−1250 nm	polycrystalline	3.3×10^{12} A m^{-2}
Lieber et al.[c]	Dia: 9 nm L: 450 nm	single crystalline	3.5×10^{12} A m^{-2}
Penner et al.[d]	W: 110−500 nm H: 10−60 nm L: ≈ 250 um	polycrystalline	$3.1\ (\pm0.7) \times 10^{11}$ A m^{-2}
bulk[e]			$\approx 10^{10}$ A m^{-2}

[a] Durkan, C.; Schneider, M. A.; Welland, M. E. *J. Appl. Phys.* **1999**, *86*, (3), 1280−1286. [b] Aherne, D.; Satti, A.; Fitzmaurice, D. *Nanotechnology* **2007**, *18*, (12), 125205. [c] Wang, C.; Hu, Y. J.; Lieber, C. M.; Sun, S. H. *J. Am. Chem. Soc.* **2008**, *130*, (28), 8902−8903. [d] This work. [e] Morris, J. W.; Kim, C. U.; Kang, S. H. *J. Met., Mater. Miner* **1996**, *48*, (5), 43−46.

size and we do not observe a progression to higher reconnection voltage thresholds with successive reconnection attempts, so this suggests that the nanogap is maintaining approximately the same mean width. But it is likely that fluctuations of the nanogap width away from this mean value are occurring and we can assume that these fluctuations eventually lead to the production of the nanogap that is too wide to undergo reconnection.

The dashed blue line in Figure 5a is an extrapolation of the initial $I-V$ curve measured for the gold nanowire before the formation of the first nanogap. These data show that the

"reconnection current" is proportional to the reconnecting voltage, on average, and that the resistance of the reconnected gold nanowire is virtually identical to the resistance of the freshly prepared gold nanowire. The progression from fresh LPNE nanowire to nanogap to reconnected nanogap is followed in the sequence of $I-V$ curves and SEM images shown in Figure 6. In this case, the resistance of the reconnected nanogap is 25% lower than the initial nanowire before electromigration, and this is due to the thermally driven grain growth that occurs during the formation of the first nanogap. Because of the limited resolution of the FE-
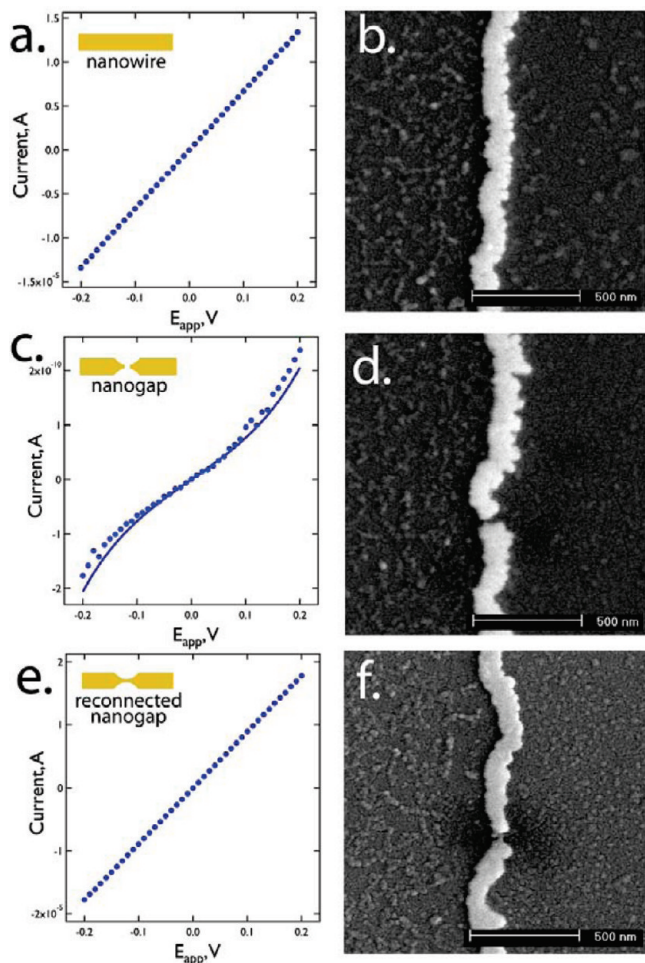
Figure 6. (a,b) $I-V$ curve (a) and SEM image (b) of a fresh gold nanowire before electromigration process. (c,d) $I-V$ curve (c) and SEM image (d) of the same nanogap after a electromigration process showing typical tunneling behavior. (e,f) SEM image (e) and SEM image (f) of the same nanogap after reconnection and electromigration.

SEM, the image of the reconnected nanogap (Figure 6f) is virtually indistinguishable from the nanogap at open circuit (Figure 6d).

Field-induced surface migration is likely responsible for the nanowire reconnection. Anaya and co-workers[25] demonstrated the formation of gold point contacts between evaporated gold contact pads across a gap with a width of 20−30 nm using field induced surface migration. The voltage pulse amplitude used to excite contact formation in that work was 10 V.[25] A similar mechanism was also proposed to account for the formation in an STM experiment of metal dots sourced by the STM tip during a voltage pulse.[26,27] This prior work has demonstrated that gold atoms, driven by strong electric fields (>1 V/Å), can be evaporated from a gold STM tip and can migrate along a surface near a nanogap. Collectively, these are exactly the behaviors required to account for the reconnection phenomenon we report here.

Failure current densities for gold nanowires fabricated by LPNE method can be calculated from the measured current during electromigration and the wire dimensions, obtained

from SEM. For ultralong gold nanowires subjected to the electromigration process for the first time, the failure current density was $3.1 \pm 0.7 \ 10^{11}$ A/m^2 (Figure 5d). Figure 5c shows a plot of failure current density for a particular gold nanowire as a function of sequential breaks. Reconnected gold nanowires fail at a much lower current density, approximately 20−25% that required to form the first nanogap. The reduced threshold for nanogap reopening supports the formation of a bow-tie-like constriction at the nanogap, also seen by SEM, that concentrates the ohmic drop along the wire axis. The gold nanowires that we investigated have a relatively low failure current density compared with other values reported in the literature previously (Table 1). These relatively low failure current densities may be partially a consequence of the extremely long wire sections probed in this study. Ohmic wire heating is dramatically enhanced in long nanowire segments, possibly promoting the electromigration process and reducing the failure current densities. Durkan and co-workers[7] derived an analytical solution for the steady-state temperature profile along the nanowire

$$T = -\frac{Q}{2km^2}e^{-mL}(e^{mx}+e^{-mx}) + Qe^{mx}\left(\frac{td}{k_{sub}} - \frac{1}{km^2}\right) + \frac{Q}{km^2} \tag{2}$$

where $Q = J^2\rho$ with J the current density and ρ its electrical resistivity, and $m = (k_{sub}/ktd)^{1/2}$. In eq 2, x is the distance measured along the nanowire from one contact, L is the wire length, k and k_{sub} are the thermal conductivities of the nanowire and substrate, respectively, and t and d are their respective thicknesses. Equation 2 predicts that the nanowire temperature is a maximum at its center, which is equidistant from the electrical contacts. Using our observed failure current densities (Table 1) and the other parameters of our experiment (with $L = 300 \ \mu$m, $t = 40$ nm, and $d = 10^{-3}$ m), this maximum temperature can exceed the melting point of gold ($T_m = 1064 \ °C$).

In summary, we have demonstrated the fabrication of sub-5 nm nanogaps within ultralong gold nanowires by a reproducible and automated, feed-back controlled electromigration process. Measurements of the resistance, applied potential, and current during electromigration show that the first nanogap formation process occurs by a somewhat different mechanism that includes the formation of a constriction located with approximately equal probability anywhere along the 250 μm electrically isolated length of the nanowire. Thermal annealing and grain growth of gold nanowires are observed during this initial electromigration process. By applying a simple voltage ramp, nanogaps can often be electrically reconnected many times. Reconnected nanowires exhibit resistances that are close to values seen in the nanowire before the first electromigration operation. At least in qualitative terms, field-induced surface migration and field evaporation are mechanisms capable of accounting for the nanowire reconnection behavior seen here.

References

(1) Yu, L. H.; Natelson, D. *Nano Lett.* **2004**, *4*, 79–83.

(2) Park, H.; Lim, A. K. L.; Alivisatos, A. P.; Park, J.; McEuen, P. L. *Appl. Phys. Lett.* **1999**, *75*, 301–303.

(3) Park, H.; Park, J.; Lim, A. K. L.; Anderson, E. H.; Alivisatos, A. P.; McEuen, P. L. *Nature (London)* **2000**, *407*, 57–60.

(4) Liang, W. J.; Shores, M. P.; Bockrath, M.; Long, J. R.; Park, H. *Nature (London)* **2002**, *417*, 725–729.

(5) Ward, D. R.; Grady, N. K.; Levin, C. S.; Halas, N. J.; Wu, Y. P.; Nordlander, P.; Natelson, D. *Nano Lett.* **2007**, *7*, 1396–1400.

(6) Baik, J. M.; Lee, S. J.; Moskovits, M. *Nano Lett.* **2009**, *9* (2), 672–676.

(7) Durkan, C.; Schneider, M. A.; Welland, M. E. *J. Appl. Phys.* **1999**, *86*, 1280–1286.

(8) Hadeed, F. O.; Durkan, C. *Appl. Phys. Lett.* **2007**, *91*, 123120.

(9) Trouwborst, M. L.; van der Molen, S. J.; van Wees, B. J. *J. Appl. Phys.* **2006**, *99*, 114316.

(10) Strachan, D. R.; Smith, D. E.; Johnston, D. E.; Park, T. H.; Therien, M. J.; Bonnell, D. A.; Johnson, A. T. *Appl. Phys. Lett.* **2005**, *86*, 043109.

(11) Esen, G.; Fuhrer, M. S. *Appl. Phys. Lett.* **2005**, *87*, 263101.

(12) Johnston, D. E.; Strachan, D. R.; Johnson, A. T. C. *Nano Lett.* **2007**, *7*, 2774–2777.

(13) Taychatanapat, T.; Bolotin, K. I.; Kuemmeth, F.; Ralph, D. C. *Nano Lett.* **2007**, *7*, 652–656.

(14) Heersche, H. B.; Lientschnig, G.; O'Neill, K.; van der Zant, H. S. J. *Appl. Phys. Lett.* **2007**, *91*, 072107.

(15) Strachan, D. R.; Smith, D. E.; Fischbein, M. D.; Johnston, D. E.; Guiton, B. S.; Drndic, M.; Bonnell, D. A.; Johnson, A. T. *Nano Lett.* **2006**, *6*, 441–444.

(16) Strachan, D. R.; Johnston, D. E.; Guiton, B. S.; Datta, S. S.; Davies, P. K.; Bonnell, D. A.; Johnson, A. T. C. *Phys. Rev. Lett.* **2008**, *100*, 056805.

(17) Xiang, C. X.; Yang, Y. A.; Penner, R. M. *Chem. Commun.* **2008**, 859–873.

(18) Xiang, C. X.; Kung, S. C.; Taggart, D. K.; Yang, F.; Thompson, M. A.; Guell, A. G.; Yang, Y. A.; Penner, R. M. *Acs Nano* **2008**, *2*, 1939–1949.

(19) Menke, E. J.; Thompson, M. A.; Xiang, C.; Yang, L. C.; Penner, R. M. *Nat. Mater.* **2006**, *5*, 914–919.

(20) Xiang, C. X.; Yang, Y. A.; Penner, R. M. *Phys. Status Solidi C* **2008**, *5*, 3503.

(21) Yang, Y.; Kung, S. C.; Taggart, D. K.; Xiang, C.; Yang, F.; Brown, M. A.; Guell, A. G.; Kruse, T. J.; Hemminger, J. C.; Penner, R. M. *Nano Lett.* **2008**, *8*, 2447–2451.

(22) Simmons, J. G. *J. Appl. Phys.* **1963**, *34*, 1793–1803.

(23) Steinmann, P.; Weaver, J. M. R. *Appl. Phys. Lett.* **2005**, *86*, 063104.

(24) Negishi, R.; Hasegawa, T.; Terabe, K.; Aono, M.; Ebihara, T.; Tanaka, H.; Ogawa, T. *Appl. Phys. Lett.* **2006**, *88*, 223111.

(25) Anaya, A.; Korotkov, A. L.; Bowman, M.; Waddell, J.; Davidovic, D. *J. Appl. Phys.* **2003**, *93*, 3501–3508.

(26) Mamin, H. J.; Guethner, P. H.; Rugar, D. *Phys. Rev. Lett.* **1990**, *65*, 2418–2421.

(27) Mayer, T. M.; Houston, J. E.; Franklin, G. E.; Erchak, A. A.; Michalske, T. A. *J. Appl. Phys.* **1999**, *85*, 8170–8177.